

Fine-grained Retrieval Prompt Tuning

Shijie Wang¹, Jianlong Chang², Zhihui Wang¹, Haojie Li^{1,3*}, Wanli Ouyang⁴, Qi Tian²

¹International School of Information Science & Engineering, Dalian University of Technology, China

²Huawei Cloud & AI, China

³College of Computer and Engineering, Shandong University of Science and Technology, China

⁴SenseTime Computer Vision Research Group, The University of Sydney, Australia

Abstract

Fine-grained object retrieval aims to learn discriminative representation to retrieve visually similar objects. However, existing top-performing works usually impose pairwise similarities on the semantic embedding spaces or design a localization sub-network to continually fine-tune the entire model in limited data scenarios, thus resulting in convergence to suboptimal solutions. In this paper, we develop Fine-grained Retrieval Prompt Tuning (FRPT), which steers a *frozen* pre-trained model to perform the fine-grained retrieval task from the perspectives of sample prompting and feature adaptation. Specifically, FRPT only needs to learn *fewer parameters* in the prompt and adaptation instead of fine-tuning the entire model, thus solving the issue of convergence to suboptimal solutions caused by fine-tuning the entire model. Technically, a discriminative perturbation prompt (DPP) is introduced and deemed as a sample prompting process, which amplifies and even exaggerates some discriminative elements contributing to category prediction via a content-aware inhomogeneous sampling operation. In this way, DPP can make the fine-grained retrieval task aided by the perturbation prompts close to the solved task during the original pre-training. Thereby, it preserves the generalization and discrimination of representation extracted from input samples. Besides, a category-specific awareness head is proposed and regarded as feature adaptation, which removes the species discrepancies in features extracted by the pre-trained model using category-guided instance normalization. And thus, it makes the optimized features only include the discrepancies among subcategories. Extensive experiments demonstrate that our FRPT with fewer learnable parameters achieves the state-of-the-art performance on three widely-used fine-grained datasets.

Introduction

Fine-grained Object Retrieval (FGOR) is to retrieve images belonging to various subcategories of a certain meta-category (*i.e.*, birds, cars and aircraft) and return images with the same subcategory as the query image. However, retrieving visually similar objects is still challenging in practical applications, especially when there exists large intra-class variances but small inter-class differences. As a result, the key to FGOR lies in learning the discriminative and generalizable embeddings to identify the visually similar objects.

Recently, the successful FGOR works fight against large intra-class but small inter-class variances by designing specialized metric constraints (Teh 2020; Wang et al. 2019a; Boudiaf et al. 2020) or locating object and even parts (Wei et al. 2017; Zheng et al. 2018; Moskvayak et al. 2021). Although metric-based and localization-based works can learn discriminative embeddings to identify fine-grained objects, the FGOR model learned from last phase is still needed to be fine-tuned on next phase endlessly, forcing the model to adapt the fine-grained retrieval task. However, continually fine-tuning the FGOR model could result in convergence to suboptimal solutions especially when facing limited-data regimes, inevitably limiting the retrieval performance (Huang et al. 2021; Zintgraf et al. 2019). Therefore, a question naturally arises: is it possible that we can still learn discriminative embeddings without fine-tuning the entire FGOR model? It is already answered yes by natural language processing (NLP) with prompt techniques.

Prompt-based learning (Liu et al. 2022) is a task-relevant instruction prepended to the input to adapt the downstream tasks to the frozen pre-trained models. Its key idea is to reformulate the downstream tasks aided by an appropriate prompt design, making it close to those solved during the original pre-training. Thereby, prompt-based learning could utilize pre-trained models directly instead of fine-tuning them to adapt downstream tasks. Following this ideology, the vision-language pre-training task has been gradually developed, which diametrically obtains visual guidance concepts from natural language via putting visual category semantics into text inputs as prompts (Jia et al. 2021; Kamath et al. 2021; Radford et al. 2021). Though these works achieve remarkable performance on many downstream vision tasks, their prompt tuning strategies are tailored for the multi-modal and thus inapplicable to fine-grained vision models. Therefore, how to devise a prompt scheme for fine-grained vision models to solve the issue of convergence to suboptimal solutions caused by fine-tuning the entire FGOR model is worthy of investigation.

To this end, we propose Fine-grained Retrieval Prompt Tuning (FRPT), which equips with discriminative perturbation prompt (DPP), pre-trained backbone model, and category-specific awareness head (CAH). FRPT merely learns fewer parameters in DPP and CAH while freezing the weights of backbone model, thus solving the convergence

*Corresponding author: hjli@dlut.edu.cn.

to suboptimal solutions. Specifically, as a sample prompting process, DPP is designed to zoom and even exaggerate some elements contributing to category prediction via a content-aware inhomogeneous sampling operation. In this way, DPP can adjust the object content towards facilitating category prediction, which makes the FGOR task prompted with this discriminative content perturbation close to the solved task during the original pre-training. Nevertheless, a non-negligible problem is that the backbone model without fine-tuning will focus on extracting features to answer the question, “*what are the different characteristics between species*” instead of “*how to distinguish fine-grained objects within the same meta-category*”. Therefore, CAH is regarded as feature adaptation to optimize the features extracted by the backbone model via removing the species discrepancies using category-guided instance normalization, thus making the optimized features only contain the discrepancies among sub-categories. Unlike fine-tuning, FRPT has fewer parameters to train, but still learns embeddings with greater discrimination and generalization owing to DPP and CAH, thus solving the convergence to suboptimal solutions caused by fine-tuning the entire model.

Our main contributions are summarized as below:

- We propose FRPT to steer a frozen pre-trained model to perform FGOR task from the perspectives of sample prompting and feature adaptation. To the best of our knowledge, we are the first to develop the prompt tuning scheme specifically for handling the convergence to suboptimal solutions caused by fine-tuning strategy in FGOR.
- A discriminative perturbation prompt is proposed to emphasize the elements contributing to decision boundary, which instructs the frozen pre-trained model to capture subtle yet discriminative details.
- A category-specific awareness head is designed to remove the discrepancies among species, which makes the features specifically for identifying fine-grained objects within the same meta-category.
- FRPT only needs to optimize about 10% of the parameters than being fully fine-tuned, and even achieves the new state-of-the-art results, *e.g.*, 3.5% average Recall@1 increase on three widely-used fine-grained retrieval datasets.

Related Work

Prompting Tuning. Prompting (Yu et al. 2022; Nie et al. 2022; Liu et al. 2022) in NLP reformulates the downstream dataset into a language modeling problem, so that a frozen language model directly adapts to a new task. Therefore, prompt tuning has now been applied to handle a variety of NLP tasks, including language understanding and generation (Lester, Al-Rfou, and Constant 2021; Li and Liang 2021; Liu et al. 2021; Jiang et al. 2020). Recently, prompt tuning has been introduced into multi-modal computer vision (Radford et al. 2021; Lin et al. 2022; Yao et al. 2021). CPT (Yao et al. 2021) converts visual grounding as the problem of filling in the blank by creating visual prompts with colored blocks and color-based textual prompts. However,

these prompt tuning based multi-modal works focus on extending the capabilities of a language-based model, inapplicable to pre-trained vision models. To fill this gap, we are the first work to develop a parameter-efficient FRPT via introducing the sample prompting and feature adaptation, thus instructing the frozen pre-trained vision model to perform FGOR task.

Fine-grained Object Retrieval: Existing FGOR methods can be roughly divided into two groups. The first group, *localization-based schemes* focuses on localizing the objects or even parts from images via exploring the activation of features (Wei et al. 2017; Zheng et al. 2018; Wang et al. 2022b; Moskvyyak et al. 2021; Wang et al. 2022a). CRL (Zheng et al. 2018) designs an attractive object feature extraction strategy to facilitate the retrieval task. Despite the inspiring achievement, the shortcoming of these works is that they only focus on discriminative embeddings while neglect the inter-class and intra-class correlations between subcategories, thus reducing the retrieval performance. Therefore, the second group, *metric-based schemes* is learning an embedding space where similar examples are attracted, and dissimilar examples are repelled (Teh 2020; Wang et al. 2019a; Boudiaf et al. 2020; Ko and Gu 2021; Roth et al. 2021; Zheng et al. 2021b). However, these existing approaches continually fine-tune the entire representation model in limited-data regimes, resulting in convergence to suboptimal solutions. To cope with this issue, FRPT attaches fewer learnable parameters into the frozen backbone network to train, instead of fine-tuning the entire representation model, but still learns discriminative embeddings.

Fine-grained Retrieval Prompt Tuning

We propose Fine-grained Retrieval Prompt Tuning (FRPT) for steering frozen pre-trained model to perform FGOR task. FRPT only optimizes fewer learnable parameters within sample prompting and feature adaptation, and keeps the backbone frozen during training. In this way, FRPT solves the issue of convergence to suboptimal solutions caused by fine-tuning the entire FGOR model.

Network Architecture

The network architecture is given in Fig. 1. Formally, given an input image I , we feed it into the discriminative perturbation prompt (DPP) module to generate the modified image I_P which selectively highlights certain elements contributing to decision boundary. After that, we take I_P as input to the frozen pre-trained backbone, and thus the semantic features M_P are outputted. To make M_P identify fine-grained objects within the same meta-category rather than recognizing diverse species, we feed M_P into the category-specific awareness head (CAH) module to generate the category-specific features M_R . Finally, the category-specific features are pass through a global average pooling operation to obtain the discriminative embeddings and then apply them to search other samples with the same subcategory.

Discriminative Perturbation Prompt

To solve the issue of convergence to suboptimal solutions caused by fine-tuning the entire model, we are inspired by

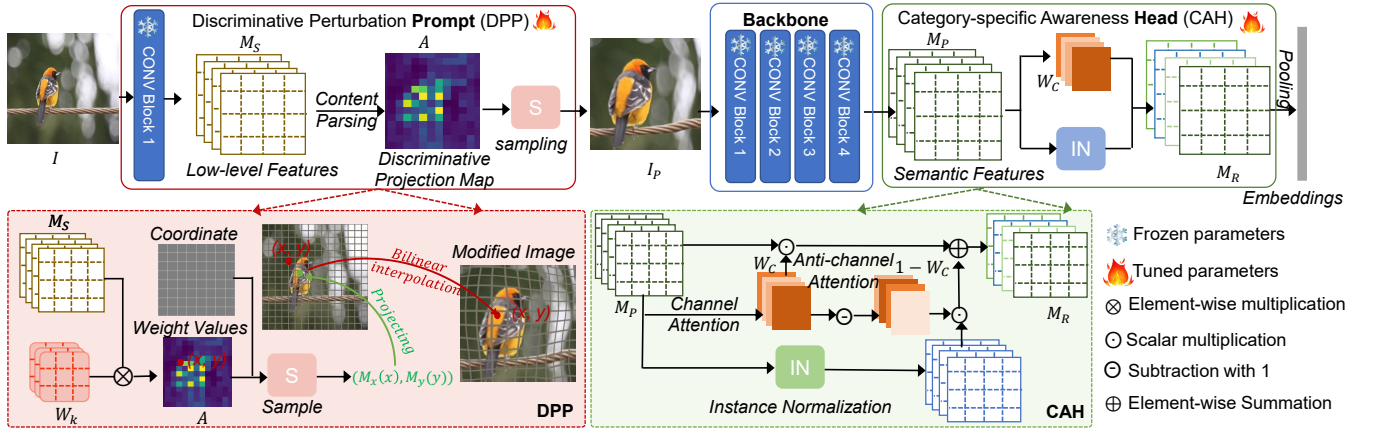


Figure 1: FRPT consists of three essential modules: the discriminative perturbation prompt module to zoom and even exaggerate the discriminative elements within objects, the frozen pre-trained backbone network to extract rich object representation, and the category-specific awareness head to compress the species discrepancies within the extracted semantic features.

prompt-based learning to solely modify the pixels in inputs, which makes the fine-grained retrieval task with the prompts close to those solved during pre-training. Therefore, we propose a discriminative perturbation prompt (DPP) module to zoom and even exaggerate some elements contributing to category prediction in the pixel space. In this way, DPP can steer the frozen pre-trained model with this perturbed prompt to perceive much more discriminative details, thus bringing the high-quality representation. Concretely, DPP consists of two steps. The first step, *content parsing*, is to learn a discriminative projection map which reflects the location and intensity of discriminative information, and the second step, *discriminative content modification*, is that zooms discriminative elements via performing the content-aware inhomogeneous sampling operation on each input image under the guidance of the discriminative projection map.

Content parsing. Perceiving details and semantics plays a vital role in perturbing the object content (Wang et al. 2020a, 2021, 2019b). Upon this, we design a content parsing module to perceive the locations and scales of discriminative semantics and details from the low-level features. The content parsing has an appealing property: large field of view that can aggregate contextual information within a large receptive field instead of exploiting pixel neighborhood. Thereby, the content parsing can capture the discriminative semantics from the low-level details while preserving the discriminative details.

Given an input image $I \in \mathbb{R}^{3 \times H \times W}$, we feed I into the convolutional block 1 of frozen pre-trained representation model \mathcal{F}_{block1} to generate the low-level features $M_S \in \mathbb{R}^{C_S \times H_S \times W_S}$, where H_S, W_S, C_S are the height, width and number of channels. It should be clarified that since the shallow layers in pre-trained representation model are sensitive to low-level details, such as color and texture, their parameters are not required to be updated and still work well.

After obtaining the low-level features M_S , we transform them into the discriminative projection map in a content-aware manner. Concretely, each target location on the dis-

criminative projection map $\mathcal{A} \in \mathbb{R}^{H_S \times W_S}$ corresponds to σ^2 source locations on M_S . Therefore, each target location shares a content-aware kernel $W_k \in \mathbb{R}^{\sigma \times \sigma \times C_S}$, where σ is the content-aware kernel size and is not less than the $\frac{1}{2}$ width of M_S , and thus is set to 31 in our experiment settings. With the shared content-aware kernel W_k , the content parsing module will specify the locations, scales and intensities of discriminative semantics and details. For a target location (m, n) , the calculation formulation is shown in Eqn. (1), where $r = \lfloor \sigma/2 \rfloor$:

$$\mathcal{A}_{(m,n)} = \sum_{w=-r}^r \sum_{h=-r}^r \sum_{c=1}^{C_S} W_k^{(w,h,c)} \cdot M_S^{(m+w,n+h,c)}. \quad (1)$$

Before being applied to the discriminative content modification operation, the discriminative projection map \mathcal{A} is normalized with a softmax function spatially. The normalization step forces the sum of the weight values in \mathcal{A} to 1:

$$\mathcal{A}_{ij} = \frac{e^{\mathcal{A}_{ij}}}{\sum_{i=1}^{W_S} \sum_{j=1}^{H_S} e^{\mathcal{A}_{ij}}}. \quad (2)$$

Discriminative content modification. This module utilizes the spatial information of sample points and corresponding sample weights in the discriminative projection map to rearrange object content, which further highlights some elements contributing to category prediction in inputs. Therefore, the modified image $I_P \in \mathbb{R}^{3 \times W \times H}$ can be formulated as below:

$$I_P = \mathcal{S}(I, \mathcal{A}), \quad (3)$$

where $\mathcal{S}(\cdot)$ indicates the content-aware inhomogeneous sampling function.

Our basic idea for inhomogeneous sampling is considering the discriminative projection map \mathcal{A} as probability mass function, where the area with large sample weight value in \mathcal{A} is more likely to be sampled. Therefore, we compute a mapping function between the modified and original images and

then use the grid sampler introduced in STN (Jaderberg et al. 2015) to rearrange objects. The mapping function can be decomposed into two dimensions, i.e., horizontal and vertical axis dimensions, thus reducing mapping complexity. Taking the coordinate (x, y) in the modified image for example, we can calculate the mapping coordinate $(\mathcal{M}_x(x), \mathcal{M}_y(y))$ in the original input as below:

$$\mathcal{M}_x(x) = \frac{\sum_{w=1}^{W_S} \sum_{h=1}^{H_S} \mathcal{A}(w, h) \cdot \mathcal{D} < (\frac{x}{W_S}, \frac{y}{H_S}), (\frac{w}{W_S}, \frac{h}{H_S}) > \cdot \frac{w}{W_S}}{\sum_{w=1}^{W_S} \sum_{h=1}^{H_S} \mathcal{A}(w, h) \cdot \mathcal{D} < (\frac{x}{W_S}, \frac{y}{H_S}), (\frac{w}{W_S}, \frac{h}{H_S}) >}, \quad (4)$$

$$\mathcal{M}_y(y) = \frac{\sum_{w=1}^{W_S} \sum_{h=1}^{H_S} \mathcal{A}(w, h) \cdot \mathcal{D} < (\frac{x}{W_S}, \frac{y}{H_S}), (\frac{w}{W_S}, \frac{h}{H_S}) > \cdot \frac{h}{H_S}}{\sum_{w=1}^{W_S} \sum_{h=1}^{H_S} \mathcal{A}(w, h) \cdot \mathcal{D} < (\frac{x}{W_S}, \frac{y}{H_S}), (\frac{w}{W_S}, \frac{h}{H_S}) >}, \quad (5)$$

where $\mathcal{D} <, >$ is a Gaussian distance kernel to act as a regularizer to avoid some extreme cases, such as all pixels converge to the same location. According to Eqn. (4)(5), we can find that that each spatial location of the modified image requires a global perspective to select the filled pixel in the original input and thus reserve the structure knowledge. In addition, the regions with large sample weight values are allocated with more sampling chances, thus zooming and even exaggerating the discriminative elements in inputs. More importantly, each pixel in the modified image is correlated with each other, and the object structure is slightly perturbed instead of being completely destroyed.

After obtaining the mapping coordinates, we then use the differentiable bi-linear sampling mechanism proposed in STN, which linearly interpolates the values of the 4-neighbors (top-left, top-right, bottom-left, bottom-right) of $(\mathcal{M}_x(x), \mathcal{M}_y(y))$ to approximate the final output, denoted by I_P ,

$$I_P(x, y) = \sum_{(i, j) \in \mathcal{N}(\mathcal{M}_x(x), \mathcal{M}_y(y))} w_p \cdot I(i, j), \quad (6)$$

where $\mathcal{N}(\mathcal{M}_x(x), \mathcal{M}_y(y))$ denotes neighbors of the mapping point $\mathcal{M}_x(x), \mathcal{M}_y(y)$ in I , and w_p is the bi-linear kernel weights estimated by the distance between the mapping point and its neighbors.

Category-specific Awareness Head

The modified image I_P is fed into the frozen pre-trained representation model to extract the semantic features $M_P \in \mathbb{R}^{C_P \times H_P \times W_P}$ derived from its last convolution layer, where H_P, W_P, C_P are the height, width, and dimension of the semantic features. However, since the semantic features extracted by the frozen pre-trained representation model aim to distinguish diverse species instead of fine-grained objects within the same meta-category, they still include some discrepancies between species, thus reducing the generalization ability of representation (Wang et al. 2020c, 2019c, 2020b). To handle this issue, we design a category-specific awareness head (CAH) to remove the species discrepancies as much as possible while only keeping the features most relevant to subcategories.

The core of CAH is Instance Normalization (IN) (Pan et al. 2018) guided by the subcategory supervision signals to remove the discrepancy among species. However, directly utilizing IN may damage discriminative information, inevitably affecting object retrieval performance. To deal with this limitation, we design a channel attention-guided IN to select the features containing the species discrepancies based on the channel-wise attention, remove them using IN, and integrate the original discriminative and optimized features into category-specific features M_R :

$$M_R = W_C \cdot M_P + (1 - W_C) \cdot IN(M_P), \quad (7)$$

where $W_C \in \mathbb{R}^{C_P}$ denotes the weight coefficients that indicates the importance of diverse channel features, and $IN(M_P)$ is the instance-normalized features of input M_P . Inspired by SENet (Hu, Shen, and Sun 2018), the channel-wise attention can be provided by

$$W_C = \Delta(W_L \delta(W_{FG}(M_P))), \quad (8)$$

where $g(\cdot)$ represents the global average pooling operation, $W_F \in \mathbb{R}^{\frac{C_P}{r} \times C_P}$ and $W_L \in \mathbb{R}^{C_P \times \frac{C_P}{r}}$ are learnable parameters in the two bias-free fully-connected layers which are followed by ReLU activation function δ and a sigmoid activation function Δ . For the dimension reduction ratio r , we aim to balance the performance and complexity and thus set it to 8. The parameter-free IN is defined as

$$IN(M_P^i) = \frac{M_P^i - E[M_P^i]}{\sqrt{Var[M_P^i] + \epsilon}}, \quad (9)$$

where $M_P^i \in \mathbb{R}^{H_P \times W_P}$ is the i -th channel of feature map M_P , ϵ is used to avoid dividing-by-zero, the mean $E[\cdot]$ and standard-deviation $Var[\cdot]$ are calculated per-channel.

It should be clarified that since the channel-wise attention in CAH is guided using the category signal y , it would determine the relevant features about the discrepancies among subcategories and the irrelevant visual patterns which do not contribute to the prediction of y . We argue that the irrelevant features do not only contain the useless discrepancies among species but also some implicitly vital information contributing to subcategory prediction. Therefore, we use IN to remove these discrepancies among species and preserve the left vital information instead of directly discarding the irrelevant features, further obtaining much better performance.

Optimization

After obtaining the category-specific features, we train the model with the cross-entropy loss merely. The following cross-entropy loss is imposed on classifier $C(\cdot)$ to predict the subcategories:

$$\mathcal{L} = -\log P(y|C(g(M_R)|\theta)), \quad (10)$$

where y denotes the label, and $C(g(M_R)|\theta)$ is the predictions of the classifier with parameters θ . The optimization process only affects the parameters within the DPP and CAH modules, but leaves no impact on backbone network during backward propagation, thus attacking the issue concerning with the convergence to suboptimal solutions owing to fine-tuning the entire representation model.

Method	Params	CUB	Cars
Pre-training (PT)	0M	44.9%	58.9%
Fine-tuning	23.53M	69.5%	84.4%
DPP + PT	0.25M	55.7%	72.7%
PT + CAH	2.62M	61.8%	76.9%
DPP + PT + CAH(w/o IN)	2.86M	72.2%	89.6%
DPP + PT + CAH	2.86M	74.3%	91.1%

Table 1: The ablative retrieval results (Recall@1) of different variants of our method. We test the models on CUB-200-2011 (CUB) and Stanford Cars (Cars). IN denotes Instance Normalization. Params denotes the numbers of learnable parameters.

Experiments

Datasets. CUB-200-2011 (Branson et al. 2014) contains 200 bird subcategories with 11,788 images. We utilize the first 100 classes (5,864 images) in training and the rest (5,924 images) in testing. The Stanford Cars (Krause et al. 2013) contains 196 car models of 16,185 images. The spilt in Stanford Cars (Krause et al. 2013) is also similar to CUB, which is split into the first 98 classes (8,045 images) for training and the remaining classes (8,131 images) for testing. FGVC Aircraft (Maji et al. 2013) is divided into first 50 classes (5,000 images) for training and the rest 50 classes (5,000 images) for testing.

Implementation Details. We apply the widely-used Resnet (He et al. 2016) in our experiments with the pre-trained parameters. The input raw images are resized to 256×256 and cropped into 224×224 . We train our models using Stochastic Gradient Descent (SGD) optimizer with weight decay of 0.0001, momentum of 0.9, and batch size of 32. We adopt the commonly used data augmentation techniques, *i.e.*, random cropping and erasing, left-right flipping, and color jittering for robust feature representations. The total number of training epochs is set to 500. Our model is relatively lightweight and is trained end-to-end on two NVIDIA 2080Ti GPUs for acceleration. The initial learning rate is set to 10^{-3} , with exponential decay of 0.9 after every 50 epochs.

Evaluation protocols. We evaluate the retrieval performance by *Recall@K* with cosine distance, which is average recall scores over all query images in the test set and strictly follows the setting in Song et al. (2016). Specifically, for each query, our model returns the top K similar images. In the top K returning images, the score will be 1 if there exists at least one positive image, and 0 otherwise.

Ablation Study

We conduct some ablation experiments to illustrate the effectiveness of the proposed modules. The baseline method uses ResNet-50 as the backbone network, followed by an Fully-Connection (FC) layer as the classifier and trained with the cross-entropy loss \mathcal{L} in the same setting. As shown in Tab. 1, the contribution of each component is revealed. We first verify the performance with freezing and fine-tuning parameters of backbone network, respectively. The results can reflect directly freezing backbone network significantly re-

duces the retrieval performance. Compared with pre-trained model, DPP only introduces few learnable parameters and improves the *Recall@1* accuracy by 10.8% and 15.8% on CUB-200-2011 and Stanford Cars datasets. The improvements also prove that DPP can instruct pre-trained models to perform fine-grained retrieval task by perturbing the object content. Additionally, we add the CAH module into the pre-trained model, bringing in 16.7% and 18.0% performance gains on two datasets. By this means that CAH could remove the species discrepancies from the features derived from pre-trained vision model, further improving retrieval results. When these two modules work together to learn discriminative embeddings, the *Recall@1* accuracy is significantly improved by 29.4% and 32.2%. Additionally, the improving performance also verifies the importance of optimizing the features containing the species discrepancies via IN rather than directly discarding them. Compared with the fine-tuning strategy, our prompt scheme has only 2.86 million learnable parameters and even suppresses fine-tuning with performance gains of 4.6% and 6.7% on two datasets, respectively. These results demonstrate that the proposed DPP and CAH can steer the frozen pre-trained model to perform the fine-grained retrieval task.

Comparison with the State-of-the-Art Methods

We compare our FRPT with state-of-the-art (SOTA) fine-grained object retrieval approaches. In Tab. 2, the performance of different methods on CUB-200-2011, Stanford Cars-196, and FGVC Aircraft datasets is reported, respectively. In the table from top to bottom, the methods are separated into three groups, which are (1) localization-based networks, (2) metric-based frameworks, and (3) our FRPT.

Existing works tend to localize object or parts to directly improve the discriminative ability of representation. Despite the encouraging achievement, the existing works still have limited ability in learning discriminative features across different subcategories due to only paying more attention to the optimization of discriminative features while overlooking the inter-class and intra-class correlations between subcategories. Therefore, the success behind these models based on deep metric learning can be largely attributed to being able to precisely identify the negative/positive pairs via enlarging/shrinking their distances, which indirectly explores the discriminative ability of features. However, these works learn discriminative embeddings via continually fine-tuning the entire representation model in limited-data regimes. We argue that this could result in convergence to suboptimal solutions and inevitably reducing model’s generalization capacity. To attack this issue, we propose FRPT to attach fewer learnable parameters of the sample prompting and feature adaptation into the frozen pre-trained model to perform the FGR task. Therefore, FRPT can achieve significantly better retrieval performance than existing works using the fine-tuning strategy.

Discussions

Effect of prompt tuning strategy. As listed in Tab. 3, fine-tuning the pre-trained vision models can degrade retrieval performance compared to freezing them. This phenomenon

Method	Arch	CUB-200-2011				Stanford Cars 196				FGVC Aircraft			
		1	2	4	8	1	2	4	8	1	2	4	8
SCDA (Wei et al.)	R50	57.3	70.2	81.0	88.4	48.3	60.2	71.8	81.8	56.5	67.7	77.6	85.7
PDDM (Bell and Bala)	R50	58.3	69.2	79.0	88.4	57.4	68.6	80.1	89.4	-	-	-	-
CRL (Zheng et al.)	R50	62.5	74.2	82.9	89.7	57.8	69.1	78.6	86.6	61.1	71.6	80.9	88.2
HDCL (Zeng et al.)	R50	69.5	79.6	86.8	92.4	84.4	90.1	94.1	96.5	71.1	81.0	88.3	93.3
DGCRL (Zheng et al.)	R50	67.9	79.1	86.2	91.8	75.9	83.9	89.7	94.0	70.1	79.6	88.0	93.0
DCML (Zheng et al.)	R50	68.4	77.9	86.1	91.7	85.2	91.8	96.0	98.0	-	-	-	-
DRML (Zheng et al.)	In3	68.7	78.6	86.3	91.6	86.9	92.1	95.2	97.4	-	-	-	-
CEP (Boudiaf et al.)	R50	69.2	79.2	86.9	91.6	89.3	93.9	96.6	98.1	-	-	-	-
MemVir (Ko and Gu)	R50	69.8	-	-	-	86.4	-	-	-	-	-	-	-
IBC (Seidenschwarz)	R50	70.3	80.3	87.6	92.7	88.1	93.3	96.2	98.2	-	-	-	-
S2SD (Roth et al.)	R50	70.1	79.7	-	-	89.5	93.9	-	-	-	-	-	-
ETLR (Kim et al.)	In3	72.1	81.3	87.6	-	89.6	94.0	96.5	-	-	-	-	-
PNCA++ (Teh)	R50	72.2	82.0	89.2	93.5	90.1	94.5	97.0	98.4	-	-	-	-
Our FRPT	R50	74.3	83.7	89.8	94.3	91.1	95.1	97.3	98.6	77.6	85.7	91.4	95.6

Table 2: Comparison of different methods on CUB-200-2011, Stanford Cars 196 and FGVC Aircraft datasets. "Arch" denotes the architecture of using backbone network. "R50" and "In3" represent Resnet50 (He et al. 2016) and Inception V3 (Szegedy et al. 2016), respectively.

Method	Arch	Params	CUB	Cars	Air
Fine-tuning	R50	23.5M	69.5	84.2	70.1
Our FRPT	R50	2.9M	74.3	91.1	77.6
Fine-tuning	R101	43.6M	70.9	85.1	69.7
Our FRPT	R101	2.9M	75.6	90.4	76.2

Table 3: Comparison of fine-tuning strategy on CUB-200-2011 (CUB), Stanford Cars 196 (Cars) and FGVC Aircraft (Air) datasets. "R50" and "R101" represent Resnet50 and Resnet101(He et al. 2016), respectively.

is reasonable since fine-tuning the pre-trained models on limited fine-grained datasets may hurt their capability of generally visual modelling due to convergence to suboptimal solutions. Additionally, our FRPT enjoys the consistent improvements on three object retrieval datasets, which validates stronger generalization ability of our sample adaptation prompts and feature adaptation head. Besides, when the pre-trained vision model is switched from Resnet50 to Resnet101, our FRPT does not introduce more learnable parameters and takes full advantage of the stronger representation power of larger models, thus resulting in the improvement of retrieval performance again. To better display the positive impact of our FRPT, we visualize the retrieval accuracy and training loss curves in Fig. 2. As can be observed from our FRPT curves, the increasing number of training epochs generally brings slow performance improvement and significantly increases the convergence speeds. One important reason of this phenomenon is that our FRPT only introduces fewer learnable parameters and thus attacks the issue concerning with convergence to the suboptimal solutions.

Effective few-shot learning. To deeper explore the effectiveness of FRPT, we conduct extensive experiments based on the few-shot setting with two different numbers of samples per subcategory: 10 and 5 on CUB-200-2011. Across

Method	Arch	Params	10-shot	5-shot
Fine-tuning	R50	23.5M	63.1%	59.7%
Our FRPT	R50	2.9M	66.6%	62.8%
Fine-tuning	R101	43.6M	64.7%	61.5%
Our FRPT	R101	2.9M	68.9%	65.2%

Table 4: Recall@1 results on CUB-200-2011 about few-shot learning. 10-shot and 5-shot indicate that only 10 and 5 images per category are used during training, respectively.

Method	R@1	R@2	R@4	R@8
CAM	63.7%	74.3%	82.5%	89.7%
Bounding box	67.6%	79.3%	85.8%	91.6%
Our DPP	74.3%	83.7%	89.8%	94.3%

Table 5: Performance comparison with other prompts in terms of Recall@K on CUB-200-2011.

the 5-shot and 10-shot experimental setting in Tab. 4, our FRPT consistently outperforms the fine-tuning strategy with different pre-trained vision models. Compared with fine-tuning pre-trained models using all images in CUB-200-2011, our FRPT only use 10 samples per subcategory but obtain the proximity performances. Since our FRPT only needs to learn a few parameters and attack the issue concerning with convergence to suboptimal solutions accordingly, our method further achieves better results than the fully fine-tuning strategy when facing only a few training samples. Therefore, the above results demonstrate the outperforming performance of FRPT owing to attaching few but effective parameters into the frozen backbone network.

Fixed prompts vs. Learnable prompts. More insight into the prompt scheme can be obtained by simple switching the processing manner of input images. As can be seen

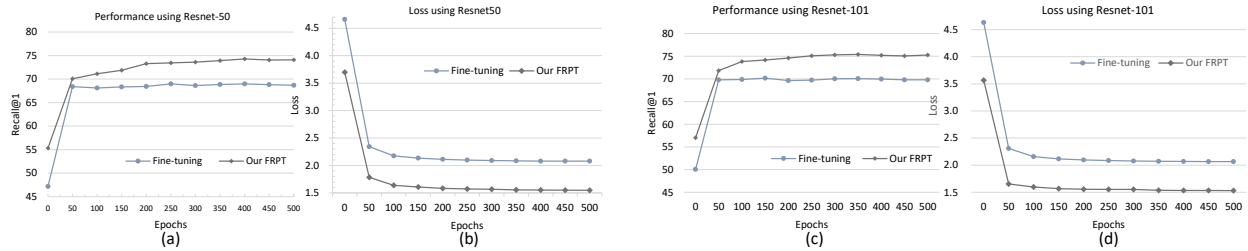


Figure 2: Curve visualization based on CUB-200-2011. (a) (c) denote the recall@1 curves about retrieval performance using Resnet-50 and Resnet-101, respectively. (b)(d) are the loss curves using Resnet-50 and Resnet-101, respectively.



Figure 3: Visualization of the object content perturbation. The first and second rows denote the original and modified images, respectively.

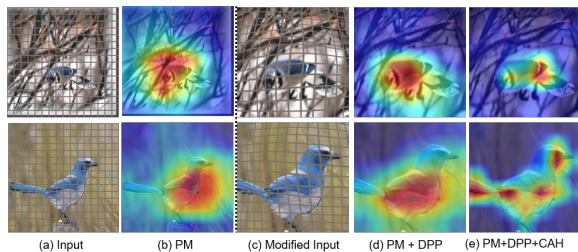


Figure 4: Illustration of class activation maps (CAM). (a)(c) are the original and modified images, respectively. (b)(d)(e) denote CAMs generated by diverse networks.

from Tab. 5, switching the processing method from the discriminative perturbation prompt (DPP) to the fixed prompt strategy, *i.e.* directly zooming objects, leads to a significant performance drop. Concretely, we use the class activation map (CAM) or the bounding boxes provided by the annotation information to localize the objects and then crop them from the original images. Tab. 5 shows a significant performance improvement when we utilize more accurate localization manner to remove the background information and preserve more object regions as much as possible. However, our FRPT zooms and even exaggerates the idiosyncratic elements contributing to decision boundary rather than to simply amplify objects and remove background, thus making the FGOR task aided by the discriminative perturbation prompt close to the solved task during the original pre-training and forming a steady improvement.

What makes a network retrieve objects visually? With this question in our mind, we exhibit the visualization re-

sults of original and modified images in Fig. 3. These visualization can interpret why and how our approach can correctly identify diverse subcategories. As shown in the second row, our sample prompting scheme can enhance the visual evidence of object parts via the dense sampling operation while suppressing the background and even non-discriminative parts, thus instructing the pre-trained model to pay more attention to discriminative details and improving the retrieval performance accordingly. It should be clarified that we manually put grid lines on the images to better display the pixel shift in the images after our prompt processing. In Fig. 4, in addition to showing the original and modified images, we present the discriminative activation maps of three representation models, *i.e.* pre-trained model (Fig. 4(b)), our FRPT without CAH (Fig. 4(d)), and our FRPT (Fig. 4(e)). It is clear that using DPP module can make the network focus on the object rather than background information, thus improving the discriminative ability of feature representation. Compared to Fig. 4(d), the activation maps (e) can pay more attention to the category-specific details via introducing CAH module. Based on these visualizations, our model generates clearer object boundaries and emphasises the discriminative details, thus providing higher retrieve performance.

Conclusion

In this paper, we propose Fine-grained Retrieval Prompt Tuning (FRPT), which aims to solve the issue of convergence to sub-optimal solutions caused by fine-tuning the entire FGOR model. FRPT design the discriminative perturbation prompt (DPP) and category-specific awareness head (CAH) to steer frozen pre-trained vision model to perform fine-grained retrieval task. Technically, DPP zooms and exaggerates some pixels contributing to category prediction, which assists the frozen pre-trained model prompted with this content perturbation to focus on discriminative details. CAH optimizes the semantic features extracted by pre-trained model via removing the species discrepancies using category-guided instance normalization, which makes the optimized features sensitive to fine-grained objects within the same meta-category. Extensive experiments demonstrate that our FRPT with fewer learnable parameters achieves the state-of-the-art performance on three widely-used fine-grained datasets.

Acknowledgements

This work is supported in part by the National Natural Science Foundation of China under Grant NO. 61976038 and NO.61932020.

References

- Bell, S.; and Bala, K. 2015. Learning visual similarity for product design with convolutional neural networks. *ACM Trans. Graph.*, 34(4): 98:1–98:10.
- Boudiaf, M.; Rony, J.; Ziko, I. M.; Granger, E.; Pedersoli, M.; Piantanida, P.; and Ayed, I. B. 2020. A Unifying Mutual Information View of Metric Learning: Cross-Entropy vs. Pairwise Losses. In Vedaldi, A.; Bischof, H.; Brox, T.; and Frahm, J., eds., *ECCV 2020*, volume 12351 of *Lecture Notes in Computer Science*, 548–564. Springer.
- Branson, S.; Horn, G. V.; Belongie, S. J.; and Perona, P. 2014. Bird Species Categorization Using Pose Normalized Deep Convolutional Nets. *CoRR*, abs/1406.2952.
- He, K.; Zhang, X.; Ren, S.; and Sun, J. 2016. Deep Residual Learning for Image Recognition. In *CVPR 2016, Las Vegas, NV, USA, June 27-30, 2016*, 770–778. IEEE Computer Society.
- Hu, J.; Shen, L.; and Sun, G. 2018. Squeeze-and-Excitation Networks. In *CVPR 2018, Salt Lake City, UT, USA, June 18-22, 2018*, 7132–7141. Computer Vision Foundation / IEEE Computer Society.
- Huang, C.; Zhai, S.; Guo, P.; and Susskind, J. M. 2021. MetricOpt: Learning To Optimize Black-Box Evaluation Metrics. In *CVPR 2021, virtual, June 19-25, 2021*, 174–183. Computer Vision Foundation / IEEE.
- Jaderberg, M.; Simonyan, K.; Zisserman, A.; and Kavukcuoglu, K. 2015. Spatial Transformer Networks. In Cortes, C.; Lawrence, N. D.; Lee, D. D.; Sugiyama, M.; and Garnett, R., eds., *Advances in Neural Information Processing Systems 28: Annual Conference on Neural Information Processing Systems 2015, December 7-12, 2015, Montreal, Quebec, Canada*, 2017–2025.
- Jia, C.; Yang, Y.; Xia, Y.; Chen, Y.; Parekh, Z.; Pham, H.; Le, Q. V.; Sung, Y.; Li, Z.; and Duerig, T. 2021. Scaling Up Visual and Vision-Language Representation Learning With Noisy Text Supervision. In Meila, M.; and Zhang, T., eds., *ICML 2021, 18-24 July 2021, Virtual Event*, volume 139 of *Proceedings of Machine Learning Research*, 4904–4916. PMLR.
- Jiang, Z.; Xu, F. F.; Araki, J.; and Neubig, G. 2020. How Can We Know What Language Models Know. *Trans. Assoc. Comput. Linguistics*, 8: 423–438.
- Kamath, A.; Singh, M.; LeCun, Y.; Synnaeve, G.; Misra, I.; and Carion, N. 2021. MDETR - Modulated Detection for End-to-End Multi-Modal Understanding. In *2021 IEEE/CVF International Conference on Computer Vision, ICCV 2021, Montreal, QC, Canada, October 10-17, 2021*, 1760–1770. IEEE.
- Kim, S.; Kim, D.; Cho, M.; and Kwak, S. 2021. Embedding Transfer With Label Relaxation for Improved Metric Learning. In *IEEE Conference on Computer Vision and Pattern Recognition, CVPR 2021, virtual, June 19-25, 2021*, 3967–3976. Computer Vision Foundation / IEEE.
- Ko, B.; and Gu, G. 2021. Learning with Memory-based Virtual Classes for Deep Metric Learning. In *2021 IEEE/CVF International Conference on Computer Vision, ICCV 2021, Montreal, QC, Canada, October 10-17, 2021*, 11772–11781. IEEE.
- Krause, J.; Stark, M.; Deng, J.; and Fei-Fei, L. 2013. 3D Object Representations for Fine-Grained Categorization. In *2013 IEEE International Conference on Computer Vision Workshops, ICCV Workshops 2013, Sydney, Australia, December 1-8, 2013*, 554–561. IEEE Computer Society.
- Lester, B.; Al-Rfou, R.; and Constant, N. 2021. The Power of Scale for Parameter-Efficient Prompt Tuning. In Moens, M.; Huang, X.; Specia, L.; and Yih, S. W., eds., *EMNLP 2021, Virtual Event / Punta Cana, Dominican Republic, 7-11 November, 2021*, 3045–3059. Association for Computational Linguistics.
- Li, X. L.; and Liang, P. 2021. Prefix-Tuning: Optimizing Continuous Prompts for Generation. In Zong, C.; Xia, F.; Li, W.; and Navigli, R., eds., *ACL/IJCNLP 2021, (Volume 1: Long Papers), Virtual Event, August 1-6, 2021*, 4582–4597. Association for Computational Linguistics.
- Lin, J.; Chang, J.; Liu, L.; Li, G.; Lin, L.; Tian, Q.; and Chen, C. W. 2022. OhMG: Zero-shot Open-vocabulary Human Motion Generation. *CoRR*, abs/2210.15929.
- Liu, L.; Yu, B. X. B.; Chang, J.; Tian, Q.; and Chen, C. W. 2022. Prompt-Matched Semantic Segmentation. *CoRR*, abs/2208.10159.
- Liu, X.; Ji, K.; Fu, Y.; Du, Z.; Yang, Z.; and Tang, J. 2021. P-Tuning v2: Prompt Tuning Can Be Comparable to Fine-tuning Universally Across Scales and Tasks. *CoRR*, abs/2110.07602.
- Maji, S.; Rahtu, E.; Kannala, J.; Blaschko, M. B.; and Vedaldi, A. 2013. Fine-Grained Visual Classification of Aircraft. *CoRR*, abs/1306.5151.
- Moskvayak, O.; Maire, F.; Dayoub, F.; and Baktashmotlagh, M. 2021. Keypoint-Aligned Embeddings for Image Retrieval and Re-identification. In *WACV 2021, Waikoloa, HI, USA, January 3-8, 2021*, 676–685. IEEE.
- Nie, X.; Ni, B.; Chang, J.; Meng, G.; Huo, C.; Zhang, Z.; Xiang, S.; Tian, Q.; and Pan, C. 2022. Pro-tuning: Unified Prompt Tuning for Vision Tasks. *CoRR*, abs/2207.14381.
- Pan, X.; Luo, P.; Shi, J.; and Tang, X. 2018. Two at Once: Enhancing Learning and Generalization Capacities via IBN-Net. In Ferrari, V.; Hebert, M.; Sminchisescu, C.; and Weiss, Y., eds., *ECCV 2018 - 15th European Conference, Munich, Germany, September 8-14, 2018, Proceedings, Part IV*, volume 11208 of *Lecture Notes in Computer Science*, 484–500. Springer.
- Radford, A.; Kim, J. W.; Hallacy, C.; Ramesh, A.; Goh, G.; Agarwal, S.; Sastry, G.; Askell, A.; Mishkin, P.; Clark, J.; Krueger, G.; and Sutskever, I. 2021. Learning Transferable Visual Models From Natural Language Supervision. In Meila, M.; and Zhang, T., eds., *ICML 2021, 18-24 July 2021, Virtual Event*, volume 139 of *Proceedings of Machine Learning Research*, 8748–8763. PMLR.

- Roth, K.; Milbich, T.; Ommer, B.; Cohen, J. P.; and Ghassemi, M. 2021. Simultaneous Similarity-based Self-Distillation for Deep Metric Learning. In Meila, M.; and Zhang, T., eds., *ICML 2021, 18-24 July 2021, Virtual Event*, volume 139 of *Proceedings of Machine Learning Research*, 9095–9106. PMLR.
- Seidenschwarz, J. D. 2021. Learning Intra-Batch Connections for Deep Metric Learning. In Meila, M.; and Zhang, T., eds., *Proceedings of the 38th International Conference on Machine Learning, ICML 2021, 18-24 July 2021, Virtual Event*, volume 139 of *Proceedings of Machine Learning Research*, 9410–9421. PMLR.
- Song, H. O.; Xiang, Y.; Jegelka, S.; and Savarese, S. 2016. Deep Metric Learning via Lifted Structured Feature Embedding. In *2016 IEEE Conference on Computer Vision and Pattern Recognition, CVPR 2016, Las Vegas, NV, USA, June 27-30, 2016*, 4004–4012. IEEE Computer Society.
- Szegedy, C.; Vanhoucke, V.; Ioffe, S.; Shlens, J.; and Wojna, Z. 2016. Rethinking the Inception Architecture for Computer Vision. In *2016 IEEE Conference on Computer Vision and Pattern Recognition, CVPR 2016, Las Vegas, NV, USA, June 27-30, 2016*, 2818–2826. IEEE Computer Society.
- Teh, E. W. 2020. ProxyNCA++: Revisiting and Revitalizing Proxy Neighborhood Component Analysis. In Vedaldi, A.; Bischof, H.; Brox, T.; and Frahm, J., eds., *Computer Vision - ECCV 2020 - 16th European Conference, Glasgow, UK, August 23-28, 2020, Proceedings, Part XXIV*, volume 12369 of *Lecture Notes in Computer Science*, 448–464. Springer.
- Wang, S.; Li, H.; Wang, Z.; and Ouyang, W. 2021. Dynamic Position-aware Network for Fine-grained Image Recognition. In *AAAI 2021, EAAI 2021, Virtual Event, February 2-9, 2021*, 2791–2799. AAAI Press.
- Wang, S.; Wang, Z.; Li, H.; and Ouyang, W. 2020a. Category-specific Semantic Coherency Learning for Fine-grained Image Recognition. In Chen, C. W.; Cucchiara, R.; Hua, X.; Qi, G.; Ricci, E.; Zhang, Z.; and Zimmermann, R., eds., *ACM MM 2020, Virtual Event / Seattle, WA, USA, October 12-16, 2020*, 174–183. ACM.
- Wang, S.; Wang, Z.; Li, H.; and Ouyang, W. 2022a. Category-Specific Nuance Exploration Network for Fine-Grained Object Retrieval. In *AAAI 2022, EAAI 2022 Virtual Event, February 22 - March 1, 2022*, 2513–2521. AAAI Press.
- Wang, S.; Wang, Z.; Wang, N.; Wang, H.; and Li, H. 2022b. From coarse to fine: multi-level feature fusion network for fine-grained image retrieval. *Multim. Syst.*, 28(4): 1515–1528.
- Wang, X.; Han, X.; Huang, W.; Dong, D.; and Scott, M. R. 2019a. Multi-Similarity Loss With General Pair Weighting for Deep Metric Learning. In *IEEE Conference on Computer Vision and Pattern Recognition, CVPR 2019, Long Beach, CA, USA, June 16-20, 2019*, 5022–5030. Computer Vision Foundation / IEEE.
- Wang, Z.; Wang, S.; Li, H.; Dou, Z.; and Li, J. 2020b. Graph-Propagation Based Correlation Learning for Weakly Supervised Fine-Grained Image Classification. In *AAAI 2020, EAAI 2020, New York, NY, USA, February 7-12, 2020*, 12289–12296. AAAI Press.
- Wang, Z.; Wang, S.; Yang, S.; Li, H.; Li, J.; and Li, Z. 2020c. Weakly Supervised Fine-Grained Image Classification via Gaussian Mixture Model Oriented Discriminative Learning. In *CVPR 2020, Seattle, WA, USA, June 13-19, 2020*, 9746–9755. IEEE.
- Wang, Z.; Wang, S.; Zhang, P.; Li, H.; and Liu, B. 2019b. Accurate And Fast Fine-Grained Image Classification via Discriminative Learning. In *ICME 2019, Shanghai, China, July 8-12, 2019*, 634–639. IEEE.
- Wang, Z.; Wang, S.; Zhang, P.; Li, H.; Zhong, W.; and Li, J. 2019c. Weakly Supervised Fine-grained Image Classification via Correlation-guided Discriminative Learning. In *ACM MM 2019, Nice, France, October 21-25, 2019*, 1851–1860.
- Wei, X.; Luo, J.; Wu, J.; and Zhou, Z. 2017. Selective Convolutional Descriptor Aggregation for Fine-Grained Image Retrieval. *IEEE Trans. Image Process.*, 26(6): 2868–2881.
- Yao, Y.; Zhang, A.; Zhang, Z.; Liu, Z.; Chua, T.; and Sun, M. 2021. CPT: Colorful Prompt Tuning for Pre-trained Vision-Language Models. *CoRR*, abs/2109.11797.
- Yu, B. X. B.; Chang, J.; Liu, L.; Tian, Q.; and Chen, C. W. 2022. Towards a Unified View on Visual Parameter-Efficient Transfer Learning. *CoRR*, abs/2210.00788.
- Zeng, X.; Liu, S.; Wang, X.; Zhang, Y.; Chen, K.; and Li, D. 2021. Hard Decorrelated Centralized Loss for fine-grained image retrieval. *Neurocomputing*, 453: 26–37.
- Zheng, W.; Wang, C.; Lu, J.; and Zhou, J. 2021a. Deep Compositional Metric Learning. In *IEEE Conference on Computer Vision and Pattern Recognition, CVPR 2021, virtual, June 19-25, 2021*, 9320–9329. Computer Vision Foundation / IEEE.
- Zheng, W.; Zhang, B.; Lu, J.; and Zhou, J. 2021b. Deep Relational Metric Learning. In *2021 IEEE/CVF International Conference on Computer Vision, ICCV 2021, Montreal, QC, Canada, October 10-17, 2021*, 12045–12054. IEEE.
- Zheng, X.; Ji, R.; Sun, X.; Wu, Y.; Huang, F.; and Yang, Y. 2018. Centralized Ranking Loss with Weakly Supervised Localization for Fine-Grained Object Retrieval. In Lang, J., ed., *IJCAI 2018, July 13-19, 2018, Stockholm, Sweden*, 1226–1233. ijcai.org.
- Zheng, X.; Ji, R.; Sun, X.; Zhang, B.; Wu, Y.; and Huang, F. 2019. Towards Optimal Fine Grained Retrieval via Decorrelated Centralized Loss with Normalize-Scale Layer. In *AAAI 2019, EAAI 2019, Honolulu, Hawaii, USA, January 27 - February 1, 2019*, 9291–9298. AAAI Press.
- Zintgraf, L. M.; Shiarlis, K.; Kurin, V.; Hofmann, K.; and Whiteson, S. 2019. Fast Context Adaptation via Meta-Learning. In Chaudhuri, K.; and Salakhutdinov, R., eds., *ICML 2019, 9-15 June 2019, Long Beach, California, USA*, volume 97 of *Proceedings of Machine Learning Research*, 7693–7702. PMLR.